A Completely New Type of Actuator
-or-
This Ain't Your Grandfather's Internal Combustion Engine

Brian W. Gore*, Gary F. Hawkins*, Peter A. Hess*, Teresa A. Moore* and Eric W. Fournier*

Abstract

A completely new type of actuator – one that is proposed for use in a variety of environments from sea to land to air to space – has been designed, patented, built, and tested. The actuator is loosely based on the principle of the internal combustion engine, except that it is a completely closed system, only requiring electrical input, and the working fuel is water. This paper outlines the theory behind the electrolysis- and ignition-based cycle upon which the actuator operates and describes the performance capability test apparatus and results for the actuator. A mechanism application that harnessed the unit's power to twist a scaled rotor blade is also highlighted.

Introduction

Traditional electro-chemical actuators use electrolysis to produce hydrogen and oxygen to generate pressure that can be used for mechanical work. These actuators can create substantial forces over large strokes but are inefficient and relatively slow. The Aerospace Corporation developed an actuator in which the hydrogen and oxygen are produced electrochemically and then ignited when actuation is desired. The process takes place in a closed volume so the water produced during combustion is contained and used again. The actuator essentially acts as a power amplifier that converts a low electrical power into stored chemical energy. The stored chemical energy can then be rapidly released (~10 ms) to produce high mechanical power in the actuator.

The advantage of this device is the extremely high energy density that can be safely stored, then delivered instantaneously. It is essentially a power amplifier – a low level of power can be input over an extended period of time, then quickly reclaimed, on the order of single-digit milliseconds. The time duration of the actuation pressure pulse can be controlled from tens of microseconds to tens of milliseconds by adding variable quantities of inert "buffer" gas, which slows down the thermal activity during combustion. In the design space of energy density vs. speed of operation, this actuator lies outside the current state-of-the-art envelope, as shown in Figure 1.

* The Aerospace Corporation, El Segundo, CA

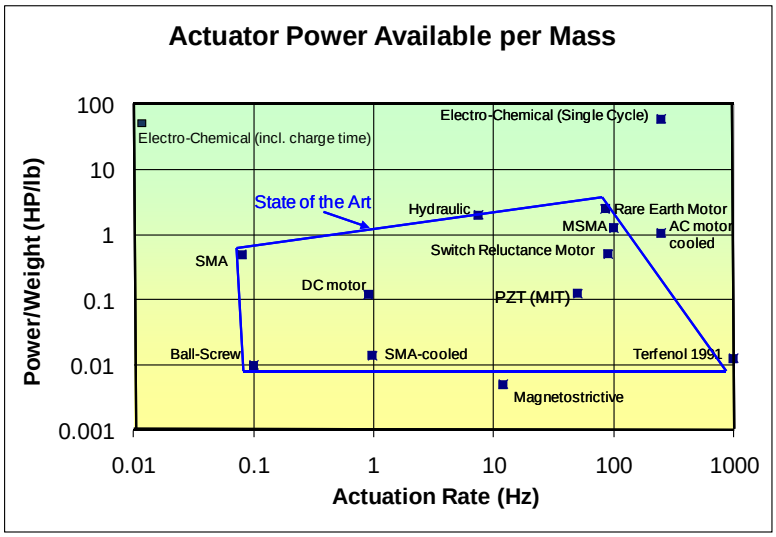

Figure 1. Actuator Specific Power vs. Actuation Rate for State Of The Art (Courtesy Of Bell Helicopter)

The heart of the closed-cell electrolysis/combustion cycle (shown in Figure 2) uses Nafion® material submerged in a small, fixed amount of water, which does not require replenishment.

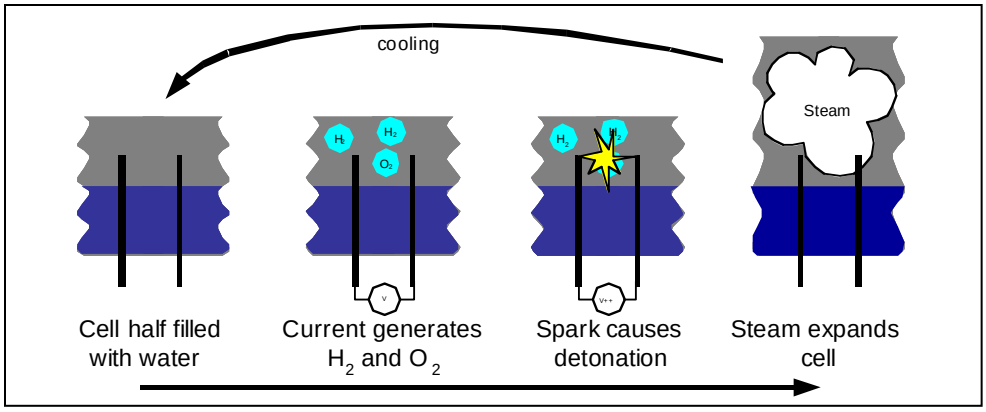

Figure 2. Schematic Drawing of the Actuation Cycle

When an electric current is passed through the Nafion®, the surrounding water undergoes electrolysis to produce hydrogen and oxygen molecules that bubble to the surface as gases. Both gases are contained within the common volume until a spark- or glow-plug is energized which then ignites the hydrogen in the system, using oxygen as the oxidizer. A large pressure pulse results from the combustion, from which mechanical work can be extracted, similar to that in a piston/cylinder system of an automobile's internal combustion engine. The difference between the two is that there is no exhaust; after combustion of the hydrogen and oxygen, the reactants are transformed into high-pressure steam that eventually condenses back into water, collecting in the reservoir. The process can continue to cycle, as long as electricity is provided to the Nafion® to drive the electrolysis.

Development of Prototype Actuator

A typical experiment during the actuator development cycle used a prototype actuator unit, shown in Figure 3, which was not optimized for weight or volume. The actuator was a piston and cylinder arrangement that pushed against a spring typically used in automotive applications. Electrolysis was performed using 7.5 W (3.75 volts and 2.0 amps) for 180 seconds, followed by ignition.

Figure 3. Piston/Cylinder Actuator (Left), And Spring It Compressed (Right) During Actuation

The resulting force and displacement profiles are shown in Figure 4. The force peaked at approximately 2.60 kN (580 lb), while pushing 1.8 cm (0.7 in) against the 145 kN/m (825 lb/in) steel compression spring. The force curve (Delta Load, in black) was measured by a load cell at the fixed end of the spring and contains additional temporal structure due to compression waves generated within the spring. The full-width-at-half-maximum duration of the force pulse was approximately 5.5 ms. Peak internal pressures of 31 MPa (4500 psi) have been attained inside the cylinder and are limited only by the strength of the cylinder itself, not the electrolysis/ignition process.

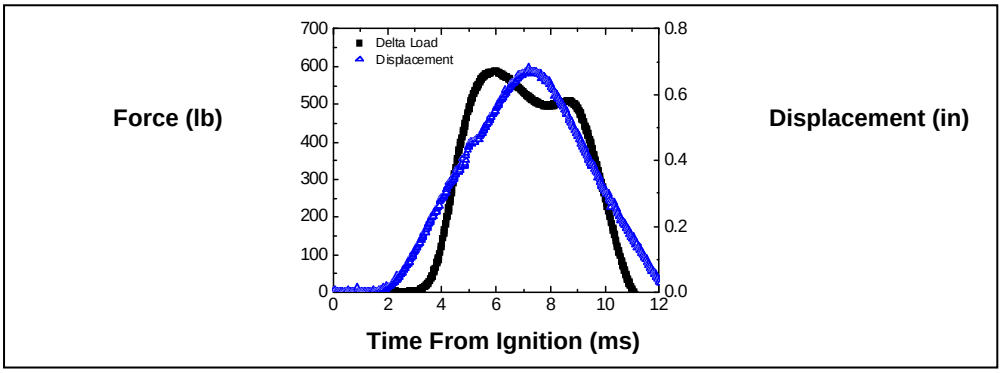

Figure 4. Load and Displacement of the Actuator Pictured in Figure 3

This example demonstrated the application of 7.5 W for 180 seconds and the achievement of >2500 W of instantaneous usable power. Again, the amount of safe potential energy stored, and power delivered, by the combusting hydrogen and oxygen is only limited by the structural integrity of the cylinder. Gas generation rate is proportional to electrolysis current; the more time-integrated current that is used, the more gas will be generated in a given time, and the more power will be available.

Development of Trigger-based Power Meter

One of the other metrics in this development effort was to determine and maximize the specific power of the actuator, with a goal of 16.7 kW/kg (50 hp/lb). Initially, the piston/cylinder pictured in Figure 3 was used with an original test “bomb” mounted to its underside as the combustion chamber (also not optimized for weight, but used readily available, off-the-shelf parts). A power density for that combination of parts – about 13.1 kW/kg (39 hp/lb) – was calculated through knowledge of pressure, surface area, and piston velocity/acceleration.

A custom, lighter-weight chamber was then designed and built for the purpose of lowering the entire Electrolysis Combustion Actuator (ECA) device’s mass, thus increasing the overall specific power density of the device. This lightweight ECA (195 g/0.43 lb) consists of a thin-walled gas generator and ignition

chamber, has ports for the igniter and buffer gas inlet, and has feed-throughs for gas generation. It replaces the original, heavy flange-based CVR (Constant Volume Reactor), (1.42 kg/3.14 lb). Figure 5 shows a close-up of the newly built, lightweight ECA chamber.

Figure 5. Lightweight Electrolysis Combustion Actuator (ECA)

A special test fixture was also developed. The fixture design needed to restrain the stroke of the piston from the build-up of pressure during the electrolysis phase, but possess a trigger function to allow the piston to begin to stroke instantly after ignition. The goal was to make this a passive device, rather than to try to incorporate a complicated feedback release system. The trigger device in Figure 6 was designed. It uses the basic principle of a quick-disconnect, ball release mechanism which will not allow relative motion until a specifically-applied external force is present; in this case, that force comes from the pressure pulse above and beyond the electrolysis static pressure. Rollers were used instead of spherical balls to allow for greater Hertzian contact load capability without brinelling. Accommodations were made for a variable-sized spacer to allow for different threshold pressures at which the device would release.

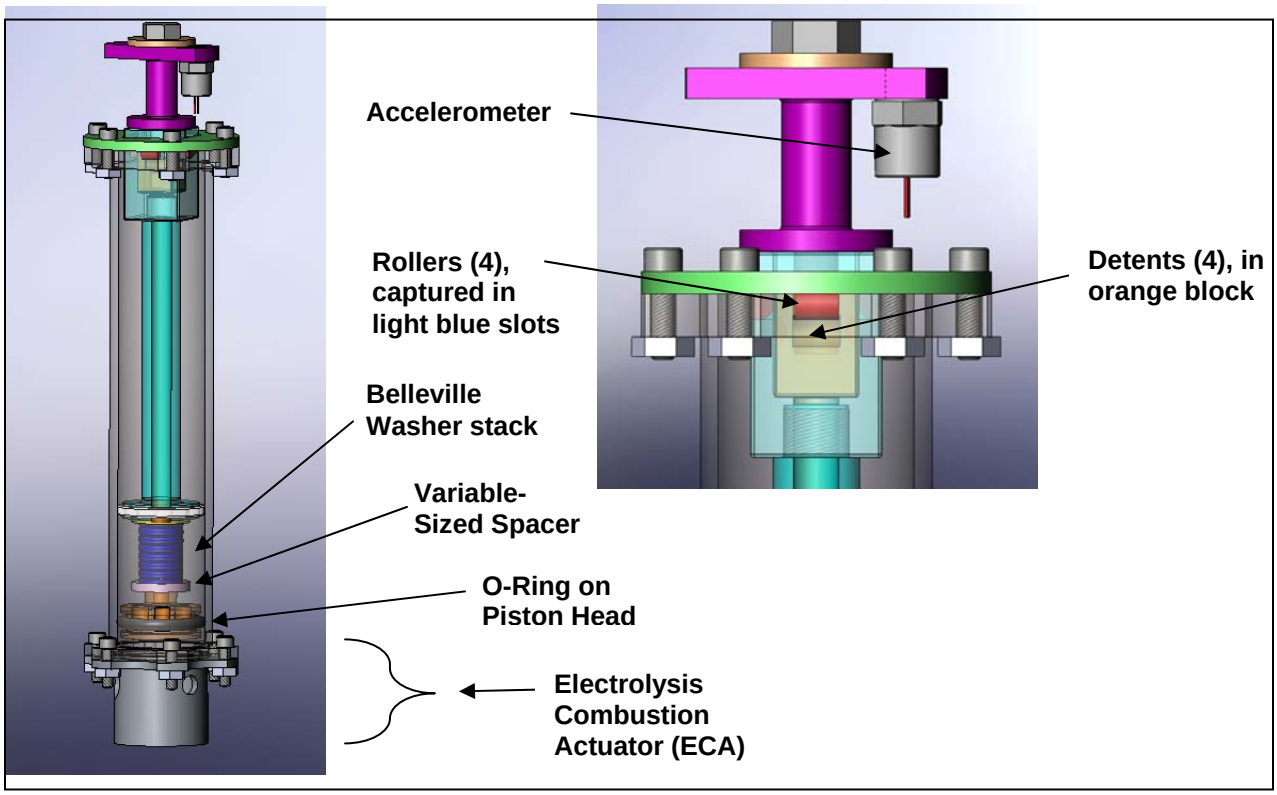

Figure 6. Quick-Disconnect Ball Release Test Fixture

The following derivation was used to calculate the horsepower being generated by the actuator on the moving mass inside the test fixture:

Power = Energy / time
Power = Force * distance / time
Power = Moving mass * acceleration * distance / time
Power = Moving mass * acceleration * velocity [1]

For the test, the moving mass in the apparatus (everything except the gray and green structural pieces) in Figure 6 was 0.2 kg (0.45 lb). The total displacement allowed before an external crushable device was impacted was 9.65 cm (3.8 in). Note that the device itself has an allowable stroke of 1.7 cm (4.6 in).

Figure 7 is a picture of the entire assembled test fixture hardware, including the ball release trigger mechanism and the ECA. Note the inclusion of the accelerometer mount at the top which serves a dual purpose as both a structural mount for the accelerometer, and also as a hard stop for the moving mass as it impacts the external crushable honeycomb unit mounted to the rigid test stand above.

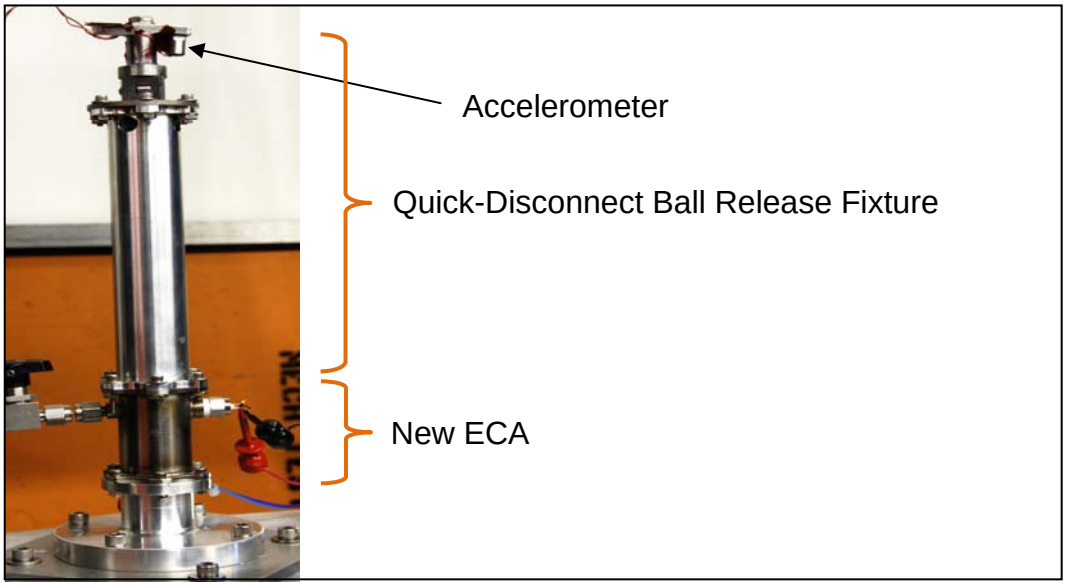

Figure 7. Complete Peak Power Density Test Fixture

Figure 8 depicts the entire test station where the specific power measurements were made. It includes the location of the test fixture on the stand, the crushable shock absorber, and the black and white measurement scale. The calibrated scale was placed behind the fixture and used as a reference to easily determine position and velocity from the high speed video camera output.

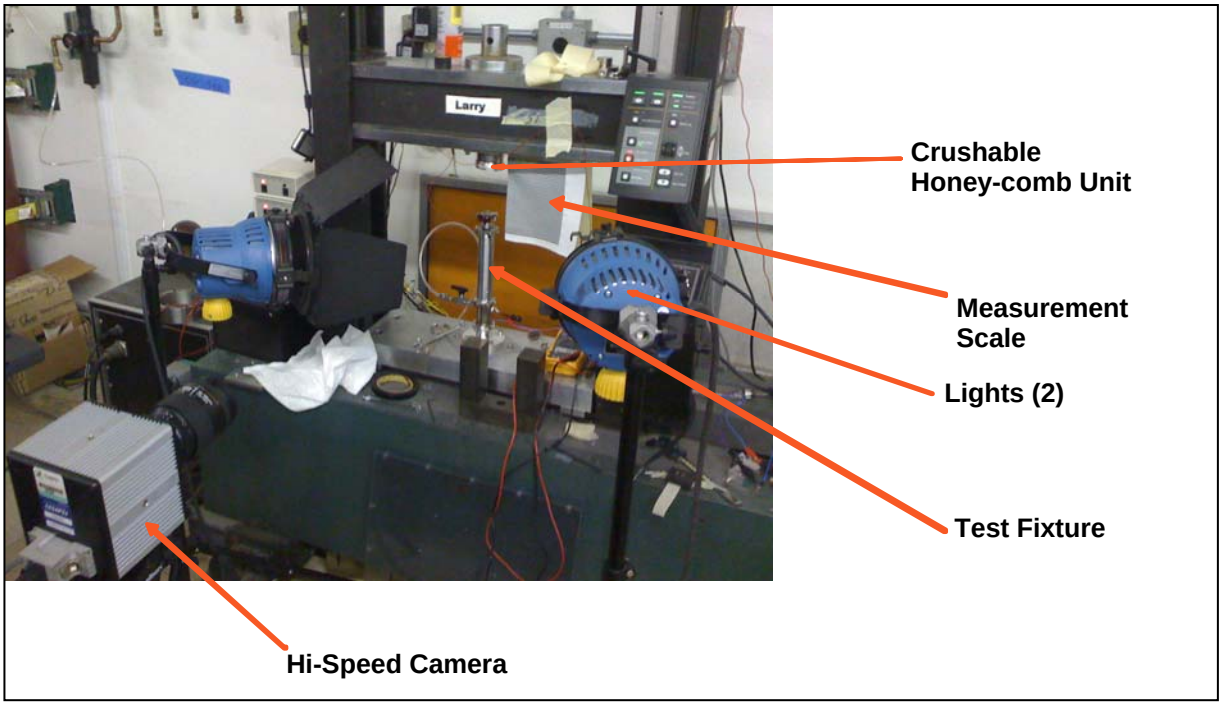

Figure 8. Peak Power Density Experimental Test Setup at The Aerospace Corporation

Figure 9 shows the first frame of the high-speed video. The accelerometer mount can be seen at the bottom of the frame, with a clear horizontal edge to use as a reference on the vertically moving part. The measurement scale is shown along the right side, and the crushable device is at the top of the frame.

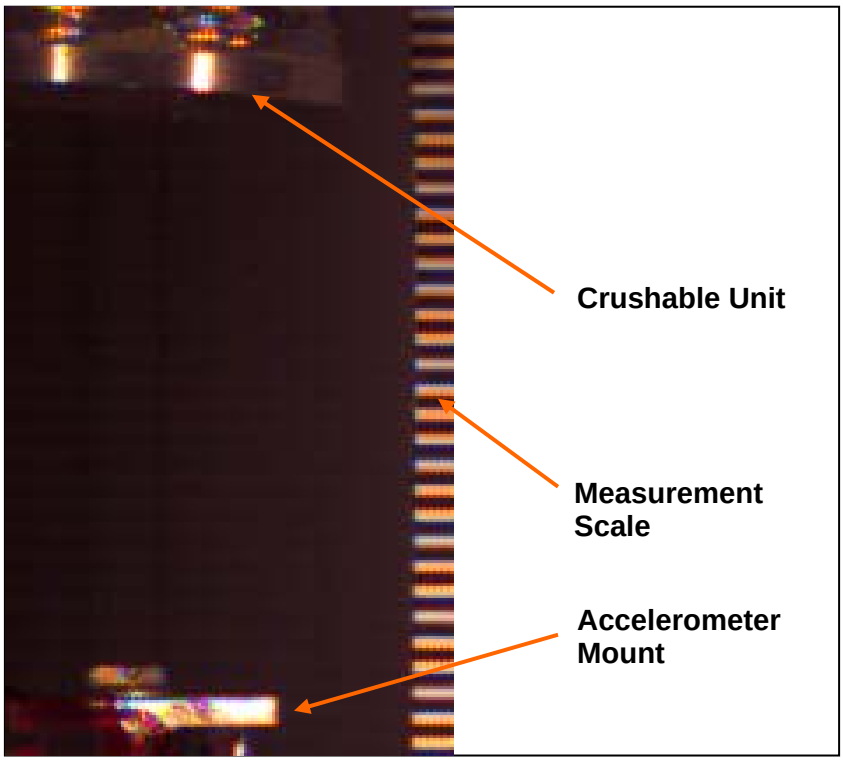

Figure 9. First Frame of Peak Power Testing High-Speed Video

Each of the measurement marks (black or white) was measured to be 2.08 mm (0.082 in) (average of many stripes divided by the number of them), and the observation points taken from the video were to count the number of marks travelled by the accelerometer stand in each frame (=0.1 ms).

The actual "run-for-record" utilized 1.38 MPa (200 psig) of argon buffer gas in the chamber, and about 0.48 MPa (70 psi) of electrolysis-generated H_2 and O_2. When combusted, the gases propelled the moving mass a distance of 9.58 cm (3.77 in) in 2.9 ms and compressed the crushable device (which had a 26–36 kN (6000-8000 lb) crush load) approximately 0.5 cm (0.2 in). That translates to an average velocity of 33 m/s (1300 in/s), which for reference is almost 119 km/hr (74 mph). The raw displacement-vs.-time data were surprisingly smooth, but when differentiated to obtain velocity and then again to obtain acceleration, the data became increasingly noisy. To solve this problem, a best-fit polynomial was found to represent the displacement-time data, which could then be more easily differentiated. Since the displacement and velocity are initially zero, the constant and first-order coefficients of a fourth-order polynomial were forced to be zero, and the result was Equation 2.

$$D = 51{,}746{,}636{,}636*t^4 - 396{,}904{,}167*t^3 + 1192091*t^2 \qquad [2]$$

where: D = displacement (in), and t = time (s)

This polynomial had an R^2 correlation of 0.9997 to the raw displacement data. With such a strong correlation factor, the best-fit method is strongly supported. The plot in Figure 10 was created after Equation 2 was differentiated for velocity and then again for acceleration. The non-zero acceleration is real, since there is a force acting on the body (from the combustion) before it starts to move.

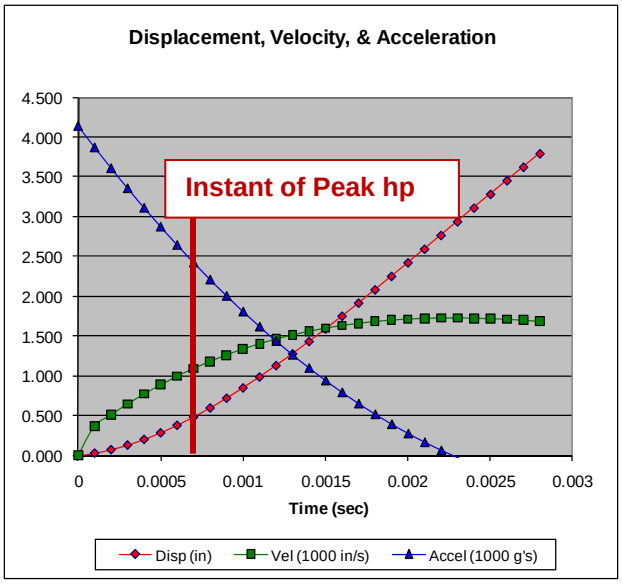

Figure 10. Displacement, Velocity, & Acceleration of Moving Mass

As illustrated in Figure 10, the peak of instantaneous horsepower occurred approximately 0.7 ms after the start of motion and was calculated, using Equation 1, to be 134 kW (180 hp). The maximum velocity achieved before the end-of-travel impact was almost 160 km/hr (100 mph). However, since the milestone to be met was specific power, not total power, that value had to be divided by the mass of the entire device that produced it. The total mass of test fixture's mechanism/cylinder (all of the hardware above the "New ECA" in Figure 7), is 0.39 kg (0.85 lb) with the moving portion at 0.20 kg (0.45 lb) and the fixed portion at 0.18 kg (0.40 lb). The mass of that ECA is 0.43 lb (the old CVR "bomb" was 1.42 kg (3.14 lb), for reference). Therefore, the calculation of the demonstrated peak specific power is

180 hp / (0.85 + 0.43) lb = 141 hp/lb (47.1 kW/kg), [3]

which was nearly triple the milestone objective of 16.7 kW/kg (50 hp/lb). Moreover, the instantaneous specific power, again using Equation 1 at each time-step, was plotted throughout the usable stroke of the test fixture, and is shown in Figure 11.

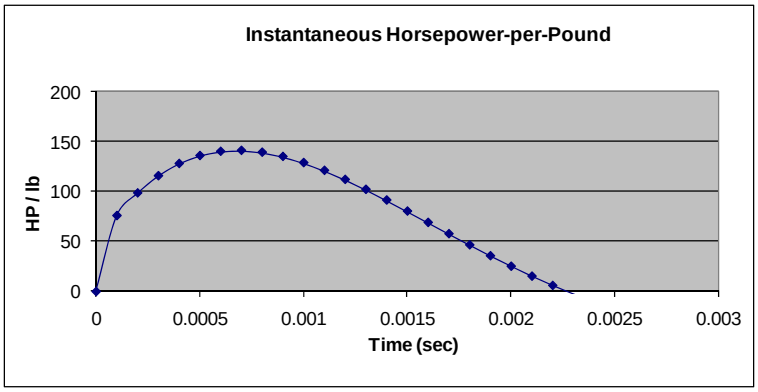

Figure 11. Specific Power Throughout Test Fixture Stroke

The important conclusion to draw from Figure 11 is that the specific power exceeded the milestone of 16.7 kW/kg (50 hp/lb) for virtually the entire effective stroke. Two different methods were originally used to curve-fit the displacement-time data, resulting in some variation in the calculation of peak power. The other method resulted in a peak of 57.1 kW/kg (171 hp/lb), or about 20% higher. The more conservative results are published here, but there should be recognition of some small level of uncertainty.

Even more power may be available with the existing setup, since only mid-sized adjustment spacers (shown in Figure 6) were used in the release/trigger mechanism; higher initial pressure (and thus final combustion pressure) could be achieved with the current hardware. Some minor fixture wear from usage was observed at this stage of the program, but nothing appeared to be detrimental to the demonstrated performance.

Practical Actuator Application Description

After proving that the state of the art in actuator technology could be exceeded, the next goal for the project was to develop a practical application for such an actuator. That application was to use the actuator, in concert with a power transfer mechanism assembly, to twist a scale prototype rotor blade. Twisting such a blade in flight was intended to improve the performance at multiple points in the performance envelope.

The actuator designed and developed for the rotor blade twist mechanism is a bidirectional electrochemical-combustive actuator designed to provide the mechanical force to twist and untwist the blade. The actuator body has mounting points and is sized to mount in the interior of the blade. The end of the piston shaft has a threaded connection to couple the actuator to the blade's internal twist mechanism. Electrical control wires extend from the actuator through the interior of the blade to its root end. Connections to external control electronics can be made from there.

The actuator design incorporates two electrochemical-combustive units that act on a single piston to provide activation in two directions. In typical blade operation the electrochemical-combustive units would be activated alternatively. One electrochemical-combustive unit serves to extend the piston shaft, while the other serves to withdraw it.

The electrochemical-combustive units operate in two phases. In the first, or "charge," phase the electrochemical unit generates combustible gas. Then in the "fire" phase, the igniter initiates the combustive process and the resulting sudden pressure pulse drives the piston, producing motion of the shaft. The force exerted by the actuator can be adjusted by varying the duration of the "charge" time.

Operation of the actuator requires power at constant current for each electrochemical unit to “charge” and power at different constant current for each igniter to “fire.”

The electrochemical-combustive units contain pressurized argon gas that modifies the combustion and heat transfer characteristics which, in turn, optimizes the transfer of energy of combustion to piston motion. The electrochemical-combustive units have valves that allow the argon pressure to be adjusted prior to initial use and during maintenance.

The electrochemical-combustive units also contain water to keep the electrochemical components submerged. In a spinning rotor blade, known water position is achieved by centrifugal force. In the testing environment, water position is achieved by orienting the actuator vertically with the piston shaft at the bottom.

Figure 12 shows a cross section of the actuator with the piston, shaft, and components of the two electrochemical-combustive units labeled. Note that the combustion chamber of the number 1 unit is above the piston, and the combustion chamber of the number 2 unit is the volume around the shaft. The volumes of these two chambers are approximately equal. The 3-D rendering on the right is shown at a slight angle to better show the piston shaft. The mounting rod, rendered in light green, is located near the bottom protruding to the right. The electrochemical units are shown in dark blue. The igniters and argon fill valves are shown in brown.

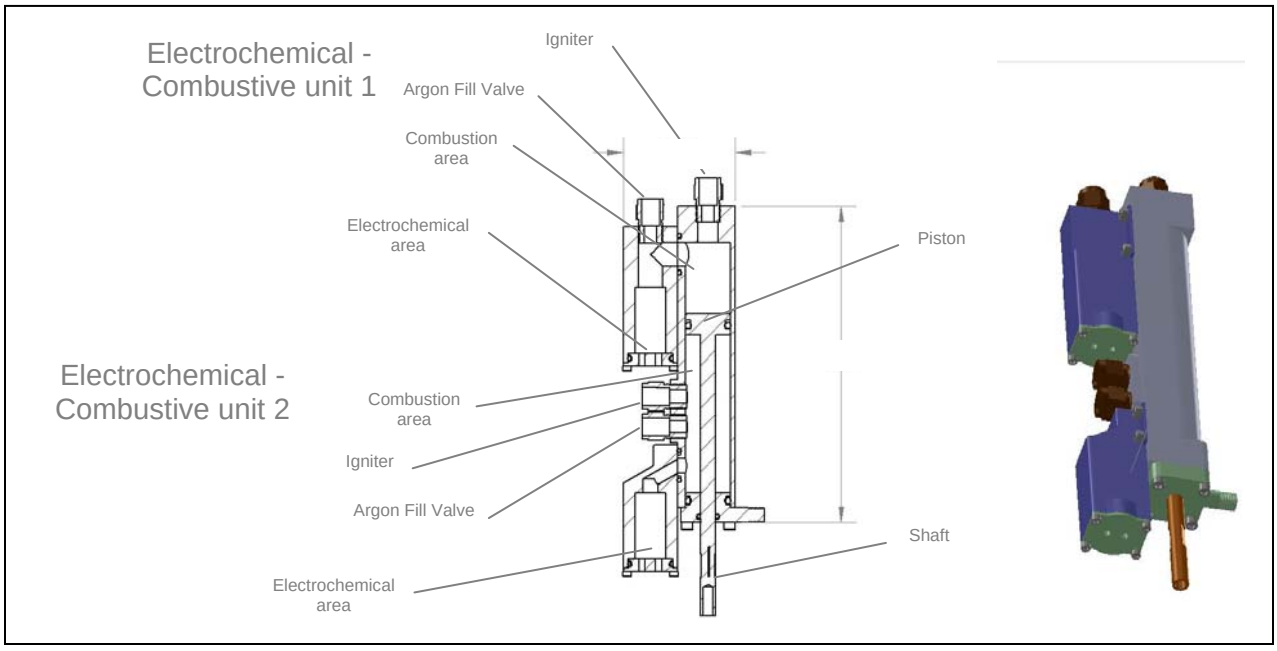

Figure 12. Bidirectional Actuator for the Rotor Blade Application

Figure 13 is a photograph of the actuator development hardware in a laboratory test stand. The photo shows black tubes and fittings connected to the argon fill valves. These valves are used to fill the electrochemical combustive units with argon and would be removed for normal operation in the blade. Note the electrical wires (white, yellow, blue) connected to each igniter and to the electrochemical areas.

Figure 13. Actuator Development Hardware in Laboratory Test Stand

Design of Twisting Tilt-Rotor Blade and Mechanism

The Aerospace Corporation's initial concepts of the rotor blade design involved a split spar and a semi-flexible trailing edge that would let the blade twist by shearing the two spar members. Since a robust design could not close around the open trailing edge, an alternative was pursued. The team noticed that shearing the two spar members also produced a slight separation between them. Using that knowledge, the team pondered that the reverse methodology should also hold, i.e., separation of the members would result in some amount of shear (and thus twist in the blade). That supposition proved to be true and is the principle that led to the design of the twist mechanism described below.

The mechanism design is based on a pin-follower, cam-based, detent shuttle concept. A CAD drawing of the mechanical system inside the blade was created, as shown in Figure 14 (some aspects not to scale).

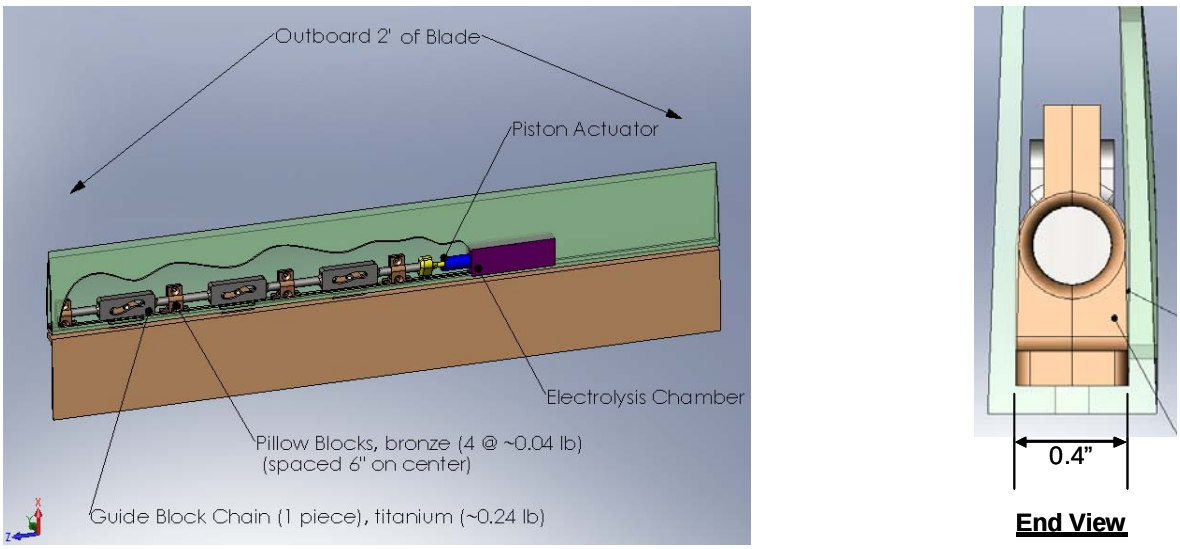

Figure 14. Preliminary CAD Representation of Twist Mechanism Inside Blade

A single actuator (in purple and blue) drives three cam mechanisms with detents in series inside the prototype blade section; the cam mechanisms, which possess respectively different profiles to produce an overall gradient deflection in the blade, are located on 15-cm (6-inch) centers to distribute the load. This preliminary design layout drawing also resulted in a first-order approximation of the size and weight of the actuator/mechanism assembly. The electrolysis/combustion team initially estimated the actuator would weigh approximately 0.2 kg (0.5 lb). Including the other masses shown in Figure 14 for which The Aerospace Corporation was responsible (actuator and power transfer mechanism), the weight goal levied for the entire subsystem was 0.45 kg (1.0 lb) plus miscellaneous attachment hardware. The weight goal was a large challenge, as one can see from the packing factor in the end view in Figure 14. The weight of the actuator development hardware shown in Figure 13 was approximately 0.59 kg (1.3 lb), which was significantly over its allocated weight. However, the mechanism portion of the assembly weighed just under its 0.2 kg (0.5 lb) allocation, so the final overall assembly weighed approximately 0.82 kg (1.8 lb).

The next step in the process was the creation of a multi-body dynamic model of the system, using Dynamic Analysis and Design System (DADS), a commercially available multi-body dynamics software. DADS aided in the evaluation of necessary actuator pressure and load to twist the rotor blade. Cam profile shapes, friction, and local blade stiffnesses were all incorporated into the model. Figure 15 shows images from the DADS model. The view is looking from the top of the blade downward, similar to Figure 14. The forward spar structure is in green (fixed reference frame), and the aft spar structure, which gets separated (and thus twists the blade via the previous discussion) is in orange. The pin (in red) is fixed to a lug mounted to the aft spar, which protrudes through an access hole in the forward spar. The actuator moves the guide blocks (shown in blue, and constrained to a fixed distance from the forward spar by pillow blocks) to the left and right. As it does so, it forces the red pin (and aft spar) fore and aft relative to the forward spar through the cam profile. In the model, the pin slides in the cam groove with an assumed friction coefficient of 0.1 (sliding but lubricated condition). Initial designs considered the inclusion of a rolling element bearing at this joint, but that option was quickly ruled out due to the very tight volume constraints and relatively large loads; Hertzian contact stresses were prohibitive. The purple model springs between the forward and aft spars represent the torsional stiffness of the blade at each cam location. Using the blade's finite element model results of applied deflections at each cam location and their respectively required forces, values were calculated for use as spring constants. Note that the three cams are slightly different in the amount of forward/aft spar separation that they produce (3.81, 2.54, and 1.27 mm (0.150, 0.100, and 0.050 in)). This separation gradient is what actually produces the twist in the blade.

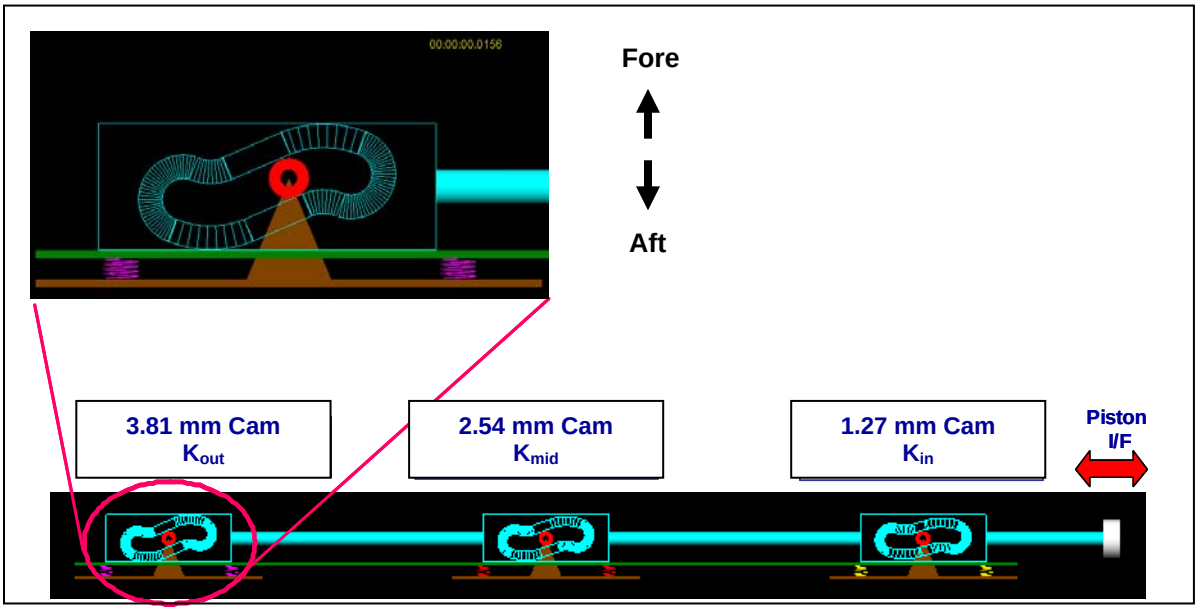

Figure 15. Screen Images of DADS Model

After the DADS model was created, several investigative runs were performed to determine the necessary force profile, specifically peak force and duration, to be delivered by the actuator. A series of spike-and-decay force pulses with a 0.002 second full-width-at-half-max (0.012 second overall) were used, since that was the general pulse shape from the actuator development testing, and the amplitude was varied. According to the simulation, a 5.17 MPa (1.47 kN) [750 psi (331 lb)] peak pulse was not successful in actuating the mechanism past the detent, but a 6.89 MPa (1000 psi) pulse was successful. With the latter pulse shape, the end-to-end actuation was predicted to be 0.004 s; a higher, 10.34 MPa (1.97 kN) [1500 psi (442 lb)] pulse was predicted to actuate in 0.002 second.

So the actuator was tuned to the correct pressure profile using appropriate levels of buffer gas and electrolysis parameters, and the tilt mechanism hardware was built. A test fixture was also built at The Aerospace Corporation to simulate the DADS model (which in turn, simulated the rotor blade) with custom-designed stacks of Belleville washers at each of the three cam locations. Given additional sources of fixture friction not accounted for in the DADS model, such as lug alignment rod sliding and pillow blocks rubbing with the connecting rods, the actual hardware and test fixture actuation time of 0.007 second was within the expected range of uncertainty. After the hardware was working satisfactorily on that fixture, it was sent to Bell Helicopter for integration into their blade, as shown in Figure 16.

A total of thirty actuations were conducted at Bell during integration bench testing, in order to properly configure the actuator with the correct electrolysis time and current, buffer gas pressure, etc. An additional thirteen actuations were conducted during the "run for record" (referred to as the Demonstration).

Three of the thirty bench test actuations ended on the up-stop (cams moving inboard in blade); and seven of the actuations ended on the down stop (cams moving outboard in blade); the remainder started or stopped somewhere in mid-stroke. There was only one bench test in which the actuator/mechanism traveled the full stroke, from up-stop to down-stop, which resulted in a total of 4 degrees of twist. This amount of twist met the goal of the project. High-speed video was used to capture the twisting events, with the beginning and ending frames showing total blade tip motion with respect to a protractor, as presented for one example in Figure 17.

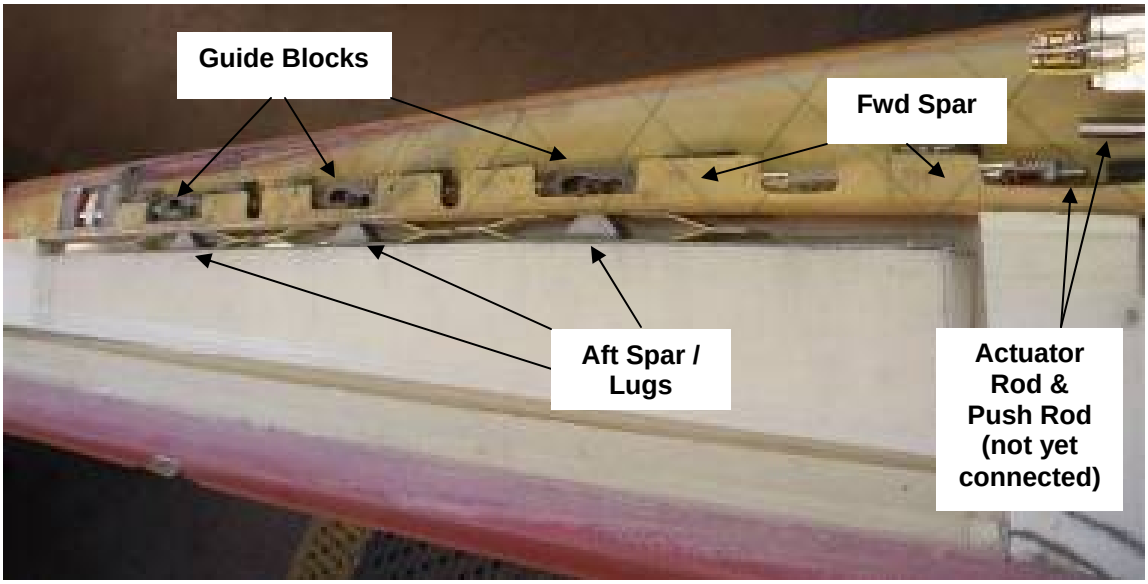

Figure 16. Cams and Rods Installed In Blade Spar Prior To Installation of Upper Skin

Once the team felt comfortable with the setup of the actuator and mechanism, the formal Demonstration for the DARPA customer was executed. Of the thirteen actuations conducted during the Demonstration, all but the first one traveled the full stroke, stop-to-stop (the first was actuated from the mid-point, since

that is the installation configuration). However, those actuations only averaged about 2.5 degrees of blade twist.

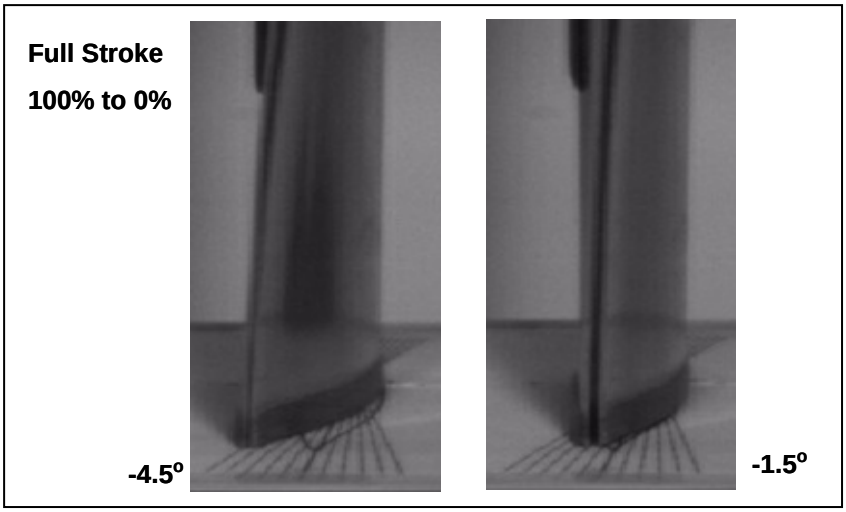

Figure 17. Beginning and End Frames from High Speed Video for Typical Sequence

After the Demonstration, the blade was X-rayed to determine if any internal failures occurred. The results, shown in Figure 18 indicate that the rods in the most outboard cam may have been previously bent. Some of the curvature seen in the X-rays is due to a "fisheye" effect because of projecting a point-source onto a flat receiver. However, the intersection of the inboard rod and Cam 1 does not appear to be perpendicular.

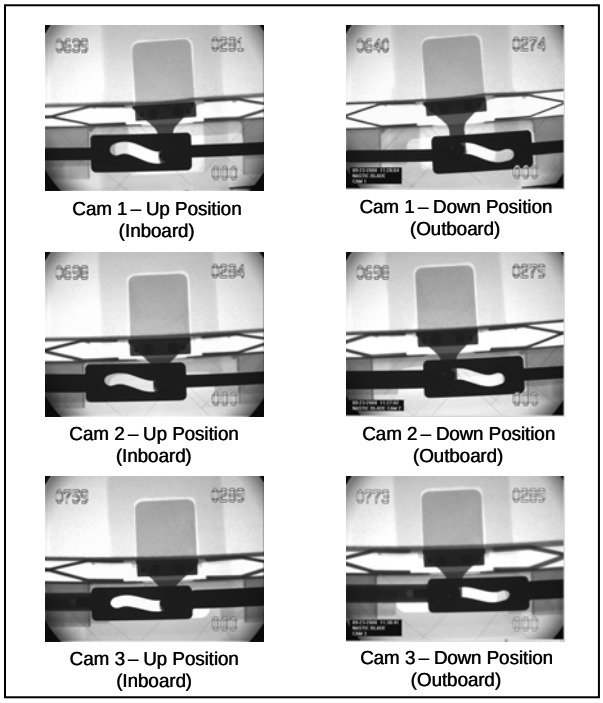

Figure 18. Post-Demonstration X-Ray Results

Post-Demonstration Evaluation

The actuator proved to have more than sufficient force to actuate the mechanism assembly. The loads in the Demonstration tended to be a little over 2.2-kN (500-lb) tension for moving the cams inboard in the blade and around 1.78-kN (400-lb) compression for moving the cams outboard. These forces are roughly what the DADS model predicted (1.5-2.0 kN (330-440 lb) minimum for a successful actuation), but are slightly higher in reality due to the additional friction features in the real hardware.

When the model used lumped masses at each of the lug locations to simulate the mass of the twisting blade, and used a pulse of 6.89 MPa (1000 psi) over 2 ms (full-width, half-max) it predicted a profile shown by the red curve in Figure 19, for actuator push rod load vs. time. That analytical curve is overlaid onto one of the successful bench test sequences for comparison.

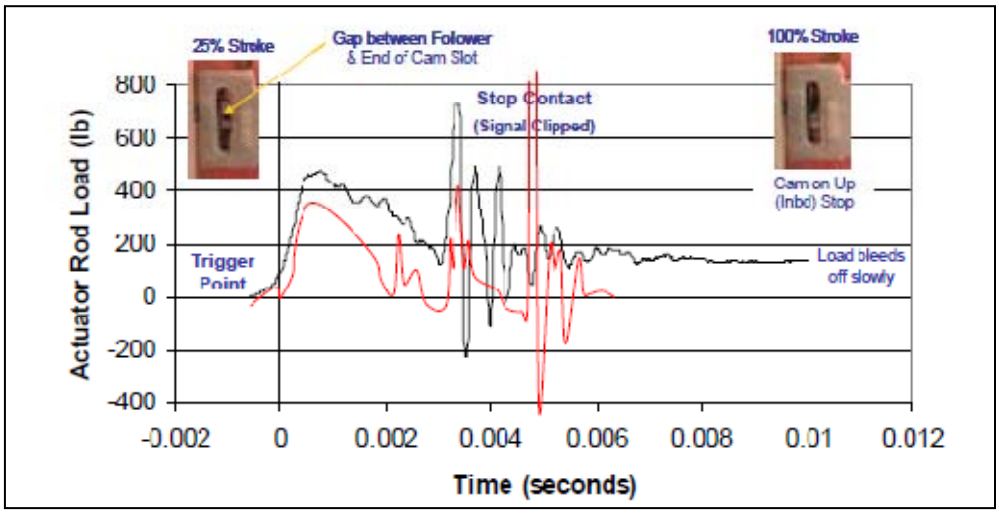

Figure 19. DADS Output (Red) Overlaid Onto Bell Test Data for Sequence 30

Lessons Learned

1. Electrolysis/combustion actuators can be used successfully to achieve a higher specific power than other currently available technologies.
2. Electrolysis time and buffer gas volume can be used to effectively tune the combustion pulse in both peak magnitude and time duration to meet specific application needs.
3. Intelligent solutions can sometimes unexpectedly result from lofty goals. The actuator goal of 16.7 kW/kg (50 hp/lb) was chosen because it was 1-2 orders of magnitude above what had ever been produced previously. Initially thought by the research team to be unattainable, that “stretch” goal drove the team to produce innovative hardware.
4. Non-metallic materials should always be part of the design trade space. Some spacecraft and launch vehicle engineers can be lulled into the familiarity of metals and their properties, but lessons can be learned from the air vehicle industry which might be just as concerned or more about light weight solutions. The pillow blocks, made out of a sintered polyamide, were a wise choice for strength, weight, and low friction.
5. Befriend the machine shop experts. Present them with reasonable designs and more importantly, reasonable deadlines. Similarly, solicit their input during the design phase, not after it has been frozen. Chances are, they have seen many different design solutions and may have different ideas to offer.

Summary/Conclusion

Extremely powerful, reusable actuators can be constructed by generating hydrogen and oxygen through electrolysis and then igniting the gas mixture when actuation is desired. The amount and rate of gas generated is simply a function of electrolysis current and time; the more Coulombs delivered, the more gas will be generated, and the more power will be available.

This technology was applied beyond the theoretical environment to achieve both goals for which the team set out to achieve. A test fixture was created to measure the instantaneous specific power of the device, which was measured at over 46.8 kW/kg (140 hp/lb), or three times the proposed goal. This result demonstrated that this type of actuator is outside the current state of actuator performance in terms of power density. Furthermore, a practical application of using such an actuator to twist a prototype rotor blade was identified, and a development actuator and power transfer mechanism were built. The goal to achieve 4 degrees of blade twist was realized with the development hardware.

Acknowledgments

The authors would like to thank the Defense Advanced Research Project Agency for their guidance and support of this research, which was part of a project led by Dr. Louis Centolanza entitled “Controllable Active Materials Via Internally Generated Pressure,” under U.S. Army Research, Development, and Engineering Command (RDECom) contract W911W6-05-C-0015. In addition, Dr. Michael J. O’Brien (materials), Aldrich R. De La Cruz (FEM modeling), and Dr. Brian M. Gable (materials and heat treating) were all instrumental in helping the project. The authors also wish to acknowledge the excellent assistance of Nolan Phillips, Ernie Powell, Joe Tzeng, and the entire Bell Helicopter partner team.